NASA Technical Memorandum 86780

Computation of Three-Dimensional Shock Wave and Boundary-Layer Interations

Ching-mao Hung

August 1985

NASA
National Aeronautics and
Space Administration

NASA Technical Memorandum 86780

Computation of Three-Dimensional Shock Wave and Boundary-Layer Interations

Ching-mao Hung, Ames Research Center, Moffett Field, California

August 1985

National Aeronautics and
Space Administration

Ames Research Center
Moffett Field, California 94035

Computation of Three-Dimensional Shock Wave And Boundary-Layer Interactions.

Ching - mao Hung*

NASA Ames Research Center
Moffett Field, California

Abstract

Computations of the impingement of an oblique shock wave on a cylinder and supersonic flow past a blunt fin mounted on a plate are used to study three-dimensional shock wave and boundary layer interaction. In the impingement case, the problem of imposing a planar impinging shock as an outer boundary condition is discussed and the details of particle traces in windward and leeward symmetry planes and near the body surface are presented. In the blunt-fin case, differences between two-dimensional and three-dimensional separation are discussed, and the existence of an unique high-speed, low-pressure region under the separated spiral-vortex core is demonstrated. The accessiblity of three-dimensional separation is discussed.

I. Introduction

In a high-Reynolds number flow, more than 95 percent of the flow is typically inviscid, and less than 5 percent, confined to a very thin layer near the boundary, is viscous. However, more than 95 percent of research effort is devoted to the problems associated with this less than 5 percent viscous region. One of the classical problems in fluid mechanics is the interaction of a shock wave with a boundary layer. A boundary layer thickens in response to the pressure increase across the shock wave. This thickening of the boundary layer shifts the shock wave forward, which in turn leads to further modification of the thickness of the boundary layer. This mutual interference is the essence of shock-wave/boundary-layer interaction.

Over the past three decades, significant effort has been devoted toward the understanding of flow phenomena of two- and three-dimensional (denoted hereafter as 2-D and 3-D for brevity) shock wave/boundary-layer interactions. Early studies began with analytical and experimental research in 2-D interactions. Recently, there have been significant advances in 3-D interaction measurements. and by a newer technique - computational studies. With the advent of supercomputers, solutions of the compressible Navier-Stokes equations for 2-D interaction problems are now obtained routinely, and computation of 3-D problems is becoming popular. The objective of a computational fluid dynamicist now is not only to calculate the flow field, but also to gain an understanding of the physics of the flow.

A computational result can be easily and quickly obtained, (say in a few CPU minutes or hours). Nevertheless, it very often explains no physics or it frequently closely predicts

*Research Scientist, Computational Fluid Dynamics Branch.

some features but not others. The purpose of this paper is to critically reassess several recently computed 3-D interaction problems, to point out certain features, to resolve some unanswered or controversial questions, and, through these, to enhance our understanding of the physics of flows and to provide information for further development and improvement of numerical flowfield simulations. The problems to be addressed are the impingement of an oblique shock wave on a cylinder (Refs. 1 and 2) and the supersonic flow past a blunt fin mounted on a plate (Refs. 3 and 4). Several related results such as flows over a sharp fin and a swept wedge will also be discussed.

II. Impingement of an Oblique Shock on a Cylinder

The impingement of an oblique shock wave on a cylindrical body is important in high-speed spacecraft design. Some realistic examples are the impingement of the bow shock from the Space Shuttle nose on the wing leading edge, the wing shock impinging on the external tank, and the store-carriage interference on a supersonic tactical aircraft. In these examples, the shock impingement results in high heating, affects the stability control, and creates force problems which could materially affect the performance of a vehicle.

A planar oblique shock wave impinging on a cylinder is illustrated schematically in Fig. 1. The shock wave is reflected from the cylinder at various angles and strengths. The inviscid flowfield at each longitudinal location is similar to that of a planar blast wave diffracting on a cylinder. Depending upon the free-stream Mach number and the incident shock angle, the incident shock may be simply reflected at the initial intersection with the cylinder. As the shock wraps around the cylinder, however, the simple reflection can no longer be sustained, and degenerates into a more complex lambda, or even double lambda structure, similar (but not identical) to observations in shock diffraction experiments. It should be pointed out that, at a large angle of incidence, no simple reflection for shock impingement can exist, even at the initial intersection with the cylinder. In this case the flow structure at longitudinal locations near the first intersection with the cylinder is no longer similar to 2-D unsteady blast wave.

This problem was investigated in Refs. 1 and 2. In these studies, time-dependent, thin-layer approximations of the 3-D Reynolds-averaged Navier-Stokes equations were solved by a mixed explicit-implicit scheme developed by MacCormack[5]. Figure 2 shows the comparison of computed and experimental surface pressure distributions along the windward and leeward symmetry generators for $M_\infty = 3.0$. The pressure contours on the cylinder surface are compared with experimentally observed levels in Fig. 3. The agreement is very good.

Figure 4 shows a comparison of the computed velocity pattern near the surface with the experimental oil-flow picture. Many features are predicted, but many others are not. The experiment indicates two oil-accumulation lines emanating from the windward plane. These oil accumulation lines are interpreted as separation lines; therefore, two separation (saddle) and two reattachment (nodal) points exist in the windward symmetry plane. The computation predicts only one separation line, and the separated region near the windward plane is substantially smaller than that shown by the experiment. Upon careful examination of the experimential oil-flow picture near the windward plane, it is difficult to see that there are two separation points. On the lee side, the inner oil-accumulation

line "seems" to split into two. Are there really two separation lines, or is there another explanation of the line of oil accumulation? This is an unanswered question. As pointed out by Dickinson[6], for flow near an appendage-plate juncture there is an inner line interpreted as a sharp demarcation between high and low shear stress regions. The existence of two separations is possible, depending on the flow condition, but the idea of a sharp demarcation between high and low shear stress or other ways of interpreting the line of oil accumulation definitely are worth further investigation.

It is difficult to describe the details of the flow structure from the experimental oil-flow pictures, especially near the leeward plane. Graphical displays of computed results show a significant advantage in this aspect. Particle traces from the computed results in the windward and leeward planes of symmetry and on the body surface are shown in Fig. 5. The flow structure in the windward symmetry plane (Fig. 5a) is separation, spiralling into a vortex, followed by reattachment. The separation and the reattachment points are not joined by a streamline; the fluid can be entrained in the separation region between the separation line and the reattachment line (a point to be discussed in more detail later). The particle traces on the body surface (Fig. 5c with detailed leeward structure in Fig. 5b) confirm the conjectured sketch of skin-friction pattern described in Ref. 1. (e.g., Fig. 11 of Ref. 1.) Along the windward generator line, there are a separation saddle and a reattachment nodal point, and along the leeward generator line, a separation node and a reattachment node. The line of cross-flow separation emanates from the saddle point near the lee side. In the leeward plane of symmetry (Fig. 5d), the line of separation lifts off from the separation node on the body surface, and there exists a singular reattachment nodal point above the body, connected to the reattachment node on the body in the leeward symmetry plane. Therefore, in the leeward symmetry plane, the fluid ahead of separation line can not flow into the separation region; the fluid is entrained outside the leeward symmetry plane into the separation region through the singular node. One remaining question is how does the flow separation structure change from the windward plane to the leeward plane? (With all the data in hand, theoretically one can construct the whole structure; but it is not an easy task.)

Note that this type of flow structure can neither be classified as a bubble-type nor as a free-vortex type separation by Maskell[7]. The flow pattern on the body (Fig. 5b) with the singular nodal point on the leeward symmetry plane (Fig. 5d), we believe, is one of many possible flow structures. Nevertheless, they are not listed as a kinematically possible combination of elementary flow structure on the body surface and in the plane of symmetry by Dallmann[8] (e.g., Fig. 7 of Ref. 8). This indicates that computations can be used to supplement experimental observations as well as theoretical studies for the investigation of the fine structure of flow fields.

From a numerical aspect, a critical point is the sharpness of the captured shock. This is a necessary condition for studying the lambda structure as the shock wraps around the cylinder. This demands a grid adaptation or a numerical scheme with high resolution. Another critical point is the way of imposing the planar shock on the outer boundary. With a uniform mesh spacing in the axial and circumferential directions, the interior mesh point will "see" the incident shock wave as a jagged surface, not a plane. This can be illustrated in a projected side view of the pre- and post-shock-wave location imposed around the outer

boundary (Fig. 6). However, a planar shock is stable; that is, if a shock is disturbed from the plane shape physically, or nonphysically, the shock tends to restore the plane shape back, with some dispersion and oscillation as it propagates. The zigzag of the imposed shock will lead to dispersion and oscillation of the flow field itself as the interior points try to "recapture" the plane shock by the numerical scheme. The problem becomes even more severe as the shock wraps around the cylinder, because the induced error propagates and accumulates downstream in a supersonic flow. (Details of this were shown in Figs. 12 and 13 of Ref. 1) The alleviation of this problem is straightforward , but not easy. These numerical considerations are also applicable to the numerical simulation of an unsteady blast wave over an object.

III. Supersonic Flow over a Blunt Fin

High speed flow over a blunt fin mounted on a surface is a typical 3-D shock-wave and boundary-layer interaction problem. The fin bow shock causes the boundary layer to separate from the surface ahead of the fin, and a reversed flow region immediately follows the separation. Above the plate, such reversed flow appears as a vortex which spirals away from the symmetry plane downstream in a typical horseshoe form. The separated flow reattaches to the plate immediately ahead of the juncture of the plate and the blunt fin. Near the root corner, there appears a small counter-rotating vortex which wraps around the fin body. The shock wave emanating from the separated flow region (separation shock) impinges on the fin bow shock, resulting in a lambda-type shock pattern ahead of the fin above the horseshoe vortex, and causes intense heating and high pressure locally around the fin leading edge.

The 3-D time-dependent Reynolds-averaged Navier-Stokes equations were solved for this flowfield using the basic MacCormack explicit-implicit predictor-corrector algorithm (Ref. 9). Details of the numerical technique are discussed in Ref. 3. The computed results are in good agreement with the pressures measured on the plate (Fig. 7) and on the fin (Fig. 8). The main features, such as peak pressure on the fin leading edge and a double peak pressure on the plate, are well predicted, and the existence of horseshoe vortices and reversed supersonic zones are displayed (see details in Ref. 4).

One of the most interesting feature observed in this flow is the role of the horseshoe vortices. First, note that the separation pattern for 2-D and the 3-D separation in the symmetry plane are completely different. These are shown in Fig. 9. In 2-D flow the separation and reattachment points, S_1 and A_1 (Fig. 9a), are connected by a dividing streamline and the region is closed. (The secondary separation, connecting S_2 and A_2, is also closed.) The separation bubble is inaccessible to the fluid outside the bubble. A fluid particle on the surface will separate at S_1, flow along the dividing streamline, and reattach at A_1. The streamlines inside are concentric. There is no mass-flux exchange between the outside and inside of the separation bubble. In 3-D flow, the separation is not closed; S_1 and A_1 are not connected by a streamline or surface. As sketched in Fig. 9b, the fluid between streamlines D and F is swept into the primary vortex and the fluid between streamlines F and C is swept into the secondary vortex. The existence of the solid wall results in an "image" or ground effect of the vortex. (The flow may be viscous, but the dominant mechanism is inviscid.) In 2-D flow, there is a similar image effect, but

there is usually insufficient momentum inside the separation bubble to show this interesting feature. In a 3-D vortex-type separation, high momentum fluid is entrained in the vortex and results in high speeds and low pressures near/on the surface under the vortex. This contributes to the existence of two reversed supersonic zones, one on the fin and another on the plate, and has led to some unexplained phenomena observed in the experiments. Indeed, this results in a significant difference between 2-D and 3-D pressure distributions on the surface. For a 2-D flow, the surface pressure typically reaches a plateau behind the separation pressure rise, and the level of the plateau pressure is based on the free interaction theory as discussed by Chapman, Kuehn and Larson[10]. In contrast to the 2-D case, a 3-D flow often exhibits a low pressure behind the separation pressure rise, the result of high speeds in the spiral vortex. It is interesting to point out that, if the flow is assumed incompressible, there is a line of zero vorticity joining the separation and reattachment points S_1 and A_1 in Fig. 9b. Definitely, this is also true for the 2-D case. It can be argued that, for incompressible flow, there is a pressure minimum ahead of separation S_1 and a pressure maximum behind the reattachment A_1.

Let's go one step further to elaborate on the accessibility of 3-D separation. Figure 10 sketches the 3-D flow structure. The separation line $S_1 - P$ emanates from the saddle point S_1; hence this separation is classified as a closed-type separation by Wang[11]. Nevertheless, as discussed above, the separation region of this type is accessible to fluid outside. In the plane of symmetry, the flow particle on the surface will lift off at the saddle point S_1 and spiral into the primary vortex. Based on the concept of limiting streamline (e.g., Ref. 12), a spiral vortex sheet is generated by an infinite number of streamlines (including the separation line $S_1 - P$ on the surface) emanating from the saddle point S_1. Strictly speaking, the fluid particle emitted from S_1 and spiraling into the vortex sheet does not reattach to the surface. It is the fluid particle along the "stream tubes" F and C that reattach to the surface. The flow particle on the surface ahead of the separation line $S_1 - P$, except on the symmetry line, can not get in to the region behind the separation line $S_1 - P$. However, the fluid above the body surface can access the separation region, because of the spiral nature of the vortex separation; some fluid goes to the primary separation and some fluid to the secondary separation. Indeed, (to our belief, but without rigorous proof), there is no 3-D separation bubble which is totally closed by a "separation surface". (We consider a perfectly axisymmetric separation as a 2-D separation.) There must be some fluid flowing in and some fluid flowing out. All 3-D separation surfaces are a kind of vortex sheet in structure.

Consider now the whole region under the horseshoe vortex. As fresh fluid is entrained into the vortex, it will accelerate to a high velocity and low pressure region above the surface under the vortex-core region. This feature is also commonly seen in vortex-generated lifting devices (e.g., Ref. 13), in flows over a cone at high angles of attack (e.g., Ref. 14), and in flows over a sharp fin (e.g., Ref. 15). Figure 11 shows comparisons of computed and measured pressure on the flat plate for flows over a sharp fin on a plate from Ref. 15, and Fig. 12 shows a result presented in Ref. 16. One can see that the strength of the vortex was underpredicted in this type of flow-field. Indeed, in Fig. 12 the calculation underpredicts the strength of two vortices, one under the shock and another close to the fin, or may even not predict the vortex near the fin at all. Supersonic flow over a swept wedge

can exhibit a similar interesting feature. Figure 13 shows recently computed and measured surface pressure distributions for a 24-degree swept wedge (Ref. 17). The two low-pressure regions with a spike in the middle are quite interesting; at first even the experimentalist (Ref. 18) doubted the measurements. This pressure is similar to that observed for the blunt-fin solution,(e.g., by combining the plot of pressure along the symmetry line on the plate and then along the fin leading edge (Figs. 7 and 8)). The first pressure rise is due to the separation. The two low-pressure regions separated by a spike in the middle are due to the image effect (on the plate and the wedge) of the vortex along the swept wedge. The last pressure peak is analogous to the peak pressure on the blunt-fin leading edge; it is caused by the reattachment of a streamline through multiple compression, instead of through just one inviscid shock compression. It might even be imagined that, with a certain combination of wedge angle, sweep angle, Mach number and Reynolds number, the spike in the middle might move away from the corner, and degenerate into multiple spikes. The computations do not have sufficient resolution to accurately describe the vortex behavior. At certain flow conditions, as the flow decelerates and the pressure begins to recover from the extreme expansion under the vortex, the reverse flow may separate and create a secondary vortex under the primary vortex. The appearance of the secondary vortex will result in a modification of surface pressure under the vortex core. This secondary vortex is often observed in flows over cones at high angles of attack and over delta wings. It is also observed in flow over a sharp fin (Ref. 19).

Two final points must be addressed; one is the numerical accuracy and another is the unsteadiness of the flow field. In the numerical aspect, the sharpness of the captured shocks and the resolution of shear layers resulting from the intersection of the separation shock on the bow shock are of principal concern. A numerical technique that can capture shocks sharply or an adaptive mesh technique is needed. Most experiments do indicate certain degrees of unsteadiness in this type of flow, as well as in other types of shock-wave and boundary-layer interactions. The observed unsteadiness is, in general, an irregular, broad-band and completely stochastic fluctuation which is associated with the dynamic nature of turbulent boundary layers. The author has tried to incorporate a time-varying, (on the order of 60 percent of the mean value), eddy viscosity model into the Reynolds-averaged Navier-Stokes equations, but results showed almost no oscillation. This suggests that the mechanism of oscillation is more complicated. The most interesting question remaining is how does the flow structure, such as the horseshoe vortex and the separation line, behave in a highly oscillatory flow field.

IV. Concluding Remarks

Computations of the impingement of a planar oblique shock wave on a cylinder and of supersonic flow over a blunt fin mounted on a plate were used to study 3-D shock wave and boundary layer interaction. In the shock impingement case, the zigzag of the imposed planar shock on the outer boundary was discussed, and the detailed particle traces in windward and leeward symmetry planes and near the body surface were presented. The question of how to interpret the experimental oil accumulation line was raised.

In the blunt fin case the differences between 2-D and 3-D separations were discussed, and the crucial feature of a high-speed, low-pressure region under the separated spiral-

vortex core was described. The concept of a closed 3-D separated region being inaccessible is valid only for the fluid on the surface, except for the line connected to the saddle point. The flow particle above the surface is able to access the separated region through the reattachment node or the vortex nature of the separation. Indeed, there is no 3-D separation bubble which is totally closed by a separation surface; there must be some fluid flowing in and some fluid flowing out. All 3-D separation surfaces are a kind of vortex sheet.

References

1. Hung, C. M.,"Impingement of an Oblique Shock Wave on a Cylinder," J. of Spacecraft and Rockets, Vol. 20, No. 3, May-June 1983, pp.201-206.

2. Brosh, A, Kussoy, M. I., and Hung, C. M.,"An Experimental and Numerical Investigation of the Impingement of an Oblique Shock Wave on a Body of Revolution," AIAA J., Vol. 23, No. 6, June 1985, pp. 840-846.

3. Hung, C. M. and Kordulla, W.,"A Time-Split Finite-Volume Algorithm for Three-Dimensional Flowfield Simulation," AIAA J., Vol. 22, No. 11, 1984, pp. 1564-1572.

4. Hung, C. M. and Buning, P. G.,"Simulation of Blunt-Fin-Induced Shock Wave and Turbulent Boundary-Layer Interaction," J. Fluid Mechanics, Vol. 154, May 1985, pp.163-185

5. MacCormack, R. W.,"An Efficient Numerical Method for Solving the Time Dependent Compressible Navier-Stokes Equations at High Reynolds Number," NASA TM X-73129, 1976.

6. Dickinson, S. C.,"Flow Visualization and Velocity Measurements in the Separated Region of an Appendage-Flat Plate Junction," The Proceedings of the Ninth Biennial Symposium on Turbulence, University of Missouri- Rolla, Oct. 1984.

7. Maskell, E. C.,"Flow Separation in Three Dimensions," RAE Rept. Aero., No. 40, 1955, pp. 11-14.

8. Dallmann, U.,"Topological Structure of Three-Dimensional Flow Separations," DFVLR-IB 221-82 A 07, 1982.

9. MacCormack, R. W.,"A Numerical Method for Solving the Equations of Compressible Viscous Flow," AIAA J., Vol. 20, Sept. 1982, pp. 1257-1281.

10. Chapman, D. R., Kuehn, D. H., and Larson, H. K.,"Investigation of Separated Flows in Supersonic and Subsonic Streams with Emphasis on the Effect of Transition," NACA Report 1356, 1958.

11. Wang, K. C.,"Separation Patterns of Boundary Layer Over An Inclined Body of Revolution," AIAA J., Vol. 10, August 1972, pp. 1044-1050.

12. Legendre, R.,"Regular or Catastrophic Evolution of Steady Flows Depending on Parameters," La Recherche Aerospatiale, No. 1982-4, 1982, pp. 42-49 (English edition)

13. Rizzetta, D. P. and Shang, J. S.,"Numerical Simulation of Leading- Edge Vortex Flows," AIAA paper No. 84-1544, July 1984.

14. Nebbleling, C. and Bannink, W. J.,"Experimental Investigation of Supersonic Flow Past a Slender Cone at High Incidence," J. of Fluid Mechanics, Vol. 87, pt. 3, 1978, pp. 475-496.

15. Knight, D. D.,"Modelling of Three-Dimensional Shock Wave/Turbulent Boundary Layer Interactions," Workshop on Macrosopic Modelling of Turbulent Flows and Fluid Mixtures, INRIA, Nice, France, Dec. 1984.

16. Hung, C. M. and MacCormack, R. W.,"Numerical Solution of Three-Dimensional Shock-Wave and Turbulent Boundary-Layer Interaction," AIAA J., Vol. 16, No. 12, Dec. 1978, pp. 1090-1096.

17. Horstman, C. C.,"A Computational Study of Complex Three-Dimensional Compressible Turbulent Flow Fields," AIAA paper No. 84-1556, July 1984.

18. Bogdonoff, S. M., Private Communications, January 1984.

19. Zheltovodov. A. A.,"Regimes and Properties of Three-Dimensional Separation Flows Initiated by Skewed Compression Shocks," Zhurnal Prikladnoi Mekhaniki i Tekhni cheskoi Fiziki, No. 3, May-June 1982, pp. 116-123.

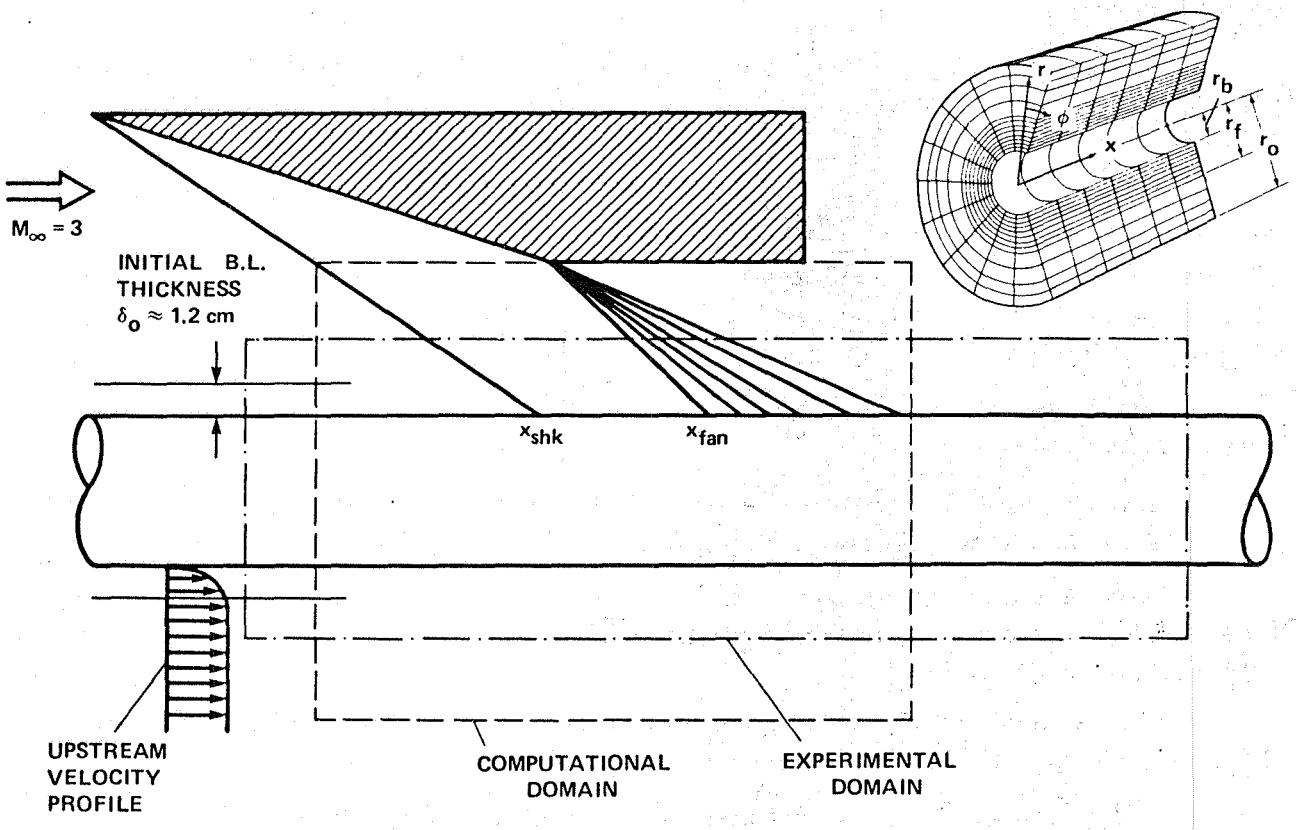

Fig. 1 Impingement of oblique shock wave on cylinder

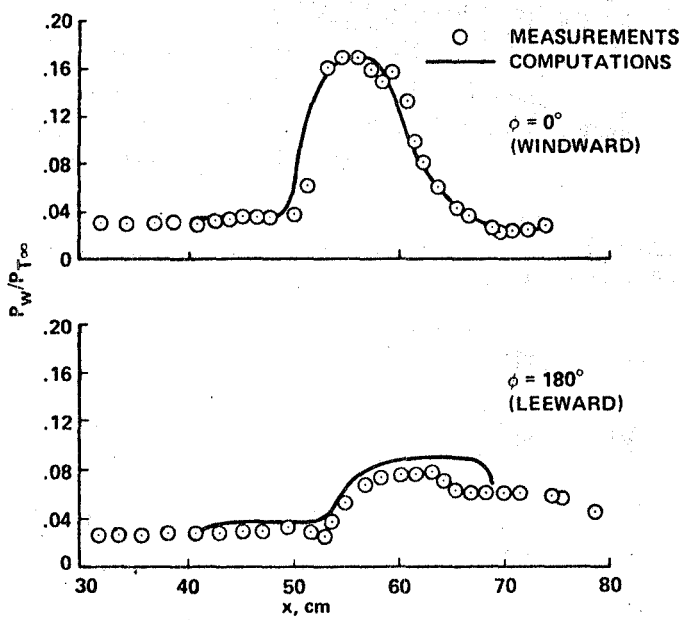

Fig. 2 Comparison of computed and experimental pressure on cylinder surface for M = 3.

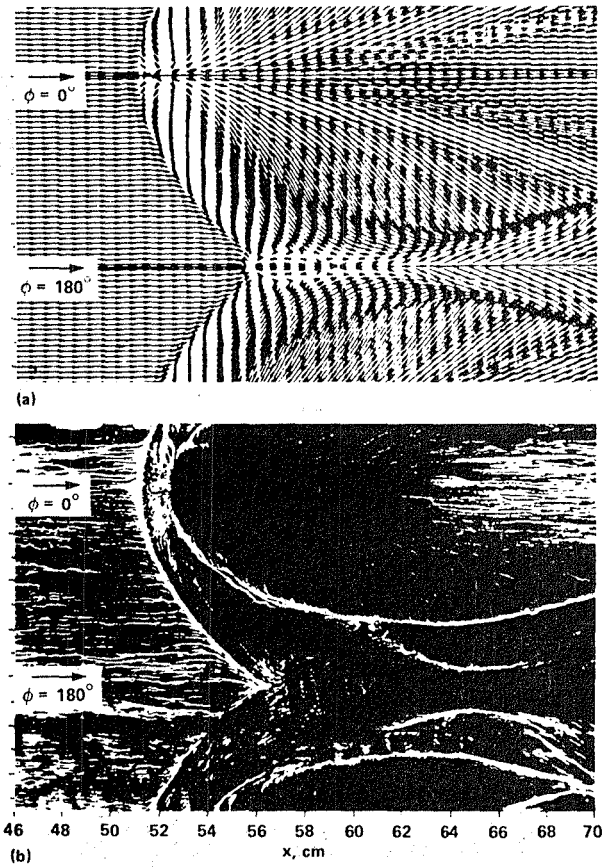

Fig. 4 Computed surface velocity pattern and experimental oil-flow picture
a) Computational; b) Experiment

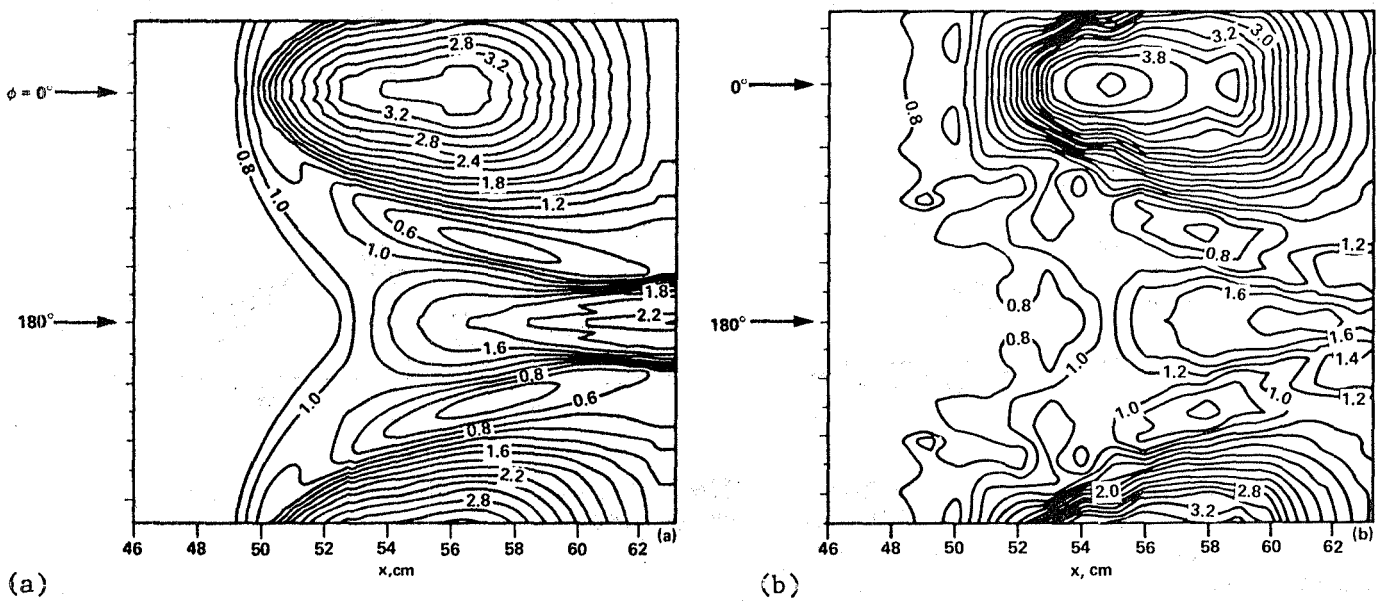

Fig. 3 Computed and experimental pressure contours on cylinder surface
a) Computed; b) Experiment

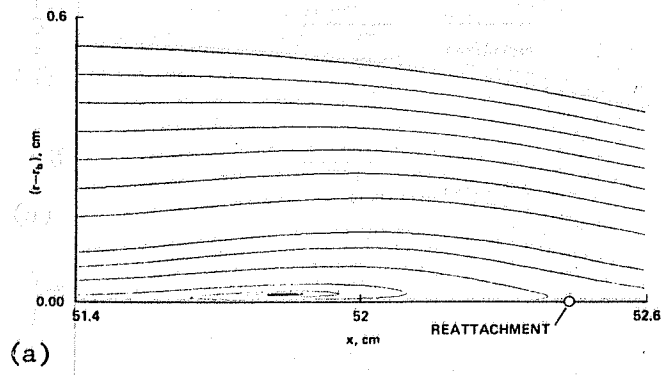

(a)

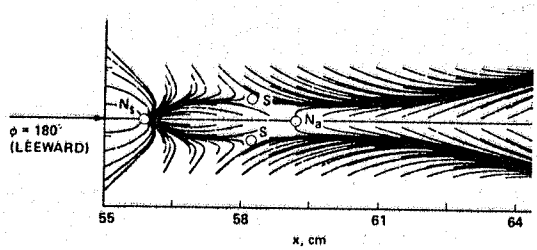

(b)

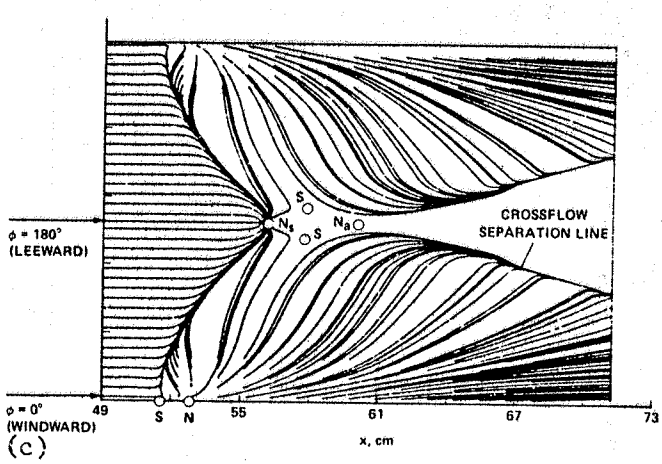

(c)

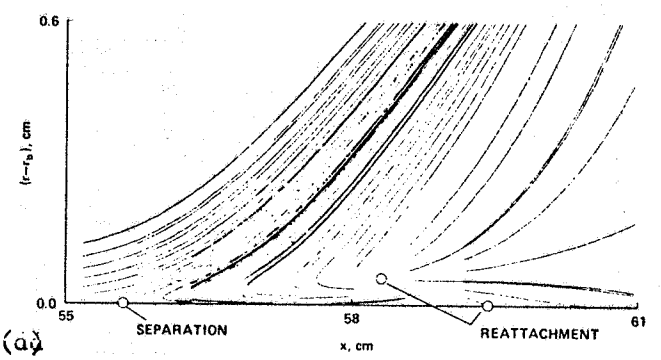

(d)

Fig. 5 Particle traces in windward and leeward symmetry planes and on cylinder. a) Windard plane; b) and c) On cylinder; d) Leeward plane.

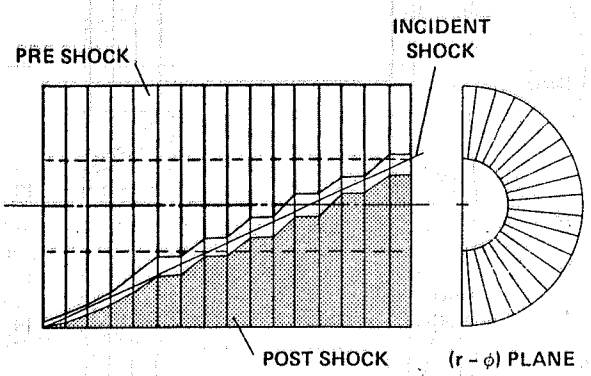

Fig. 6 Sideview of pre- and post-shock wave location at outer boundary.

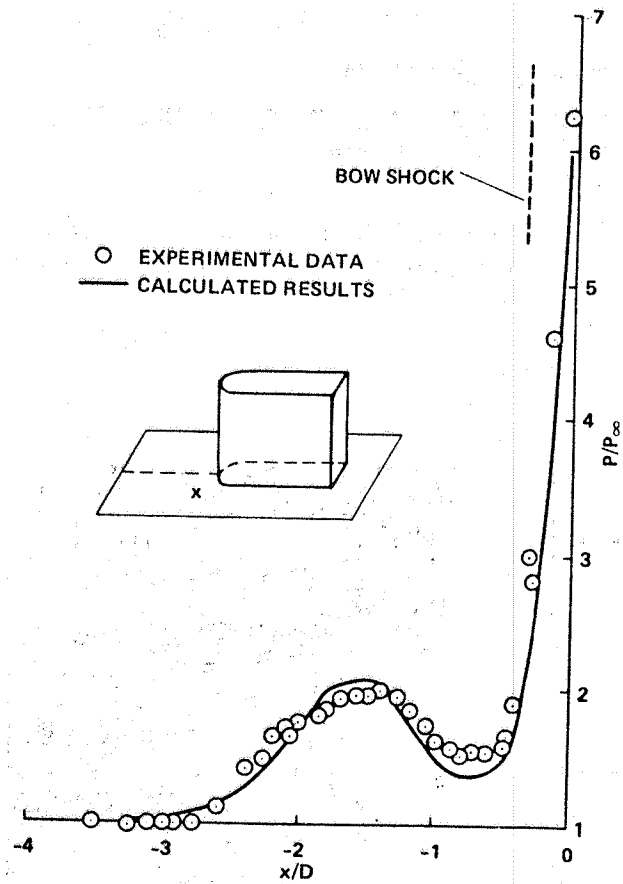

Fig. 7 Pressure on flat plate along line of symmetry.

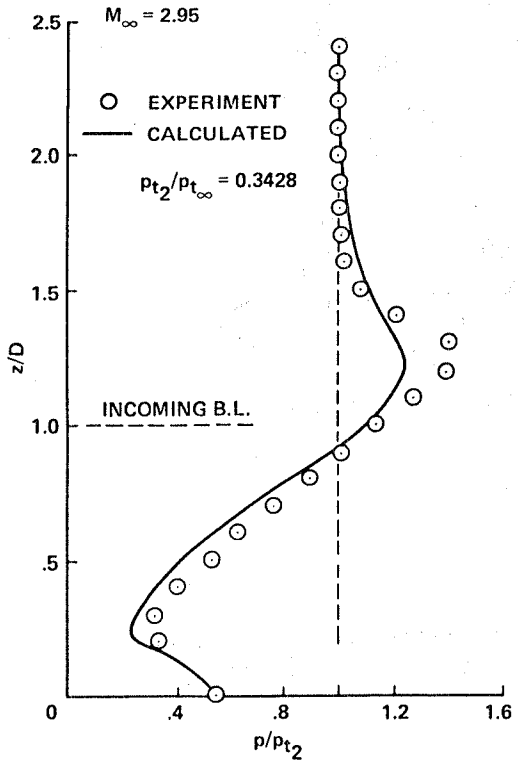

Fig. 8 Pressure along fin leading edge

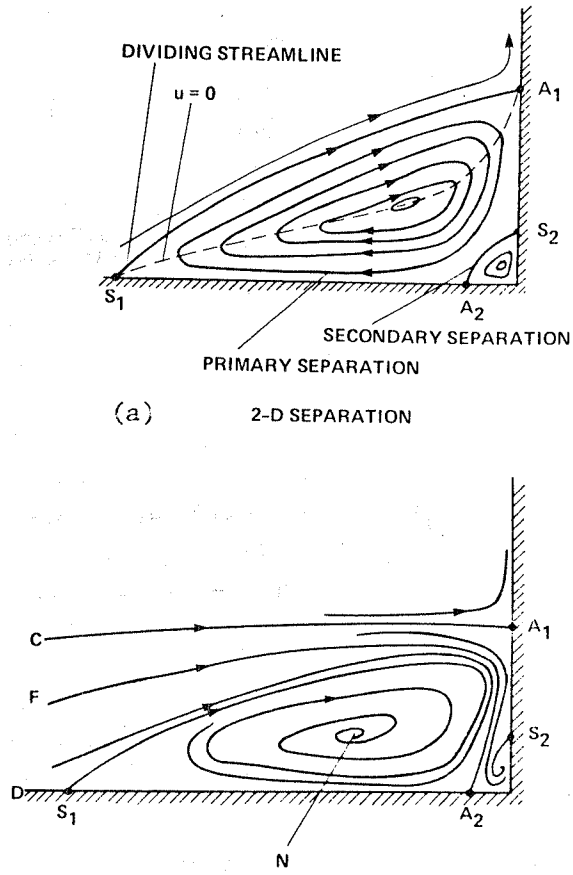

Fig. 9 Differences between 2-D and 3-D separation. a) 2-D separation; b) 3-D separation

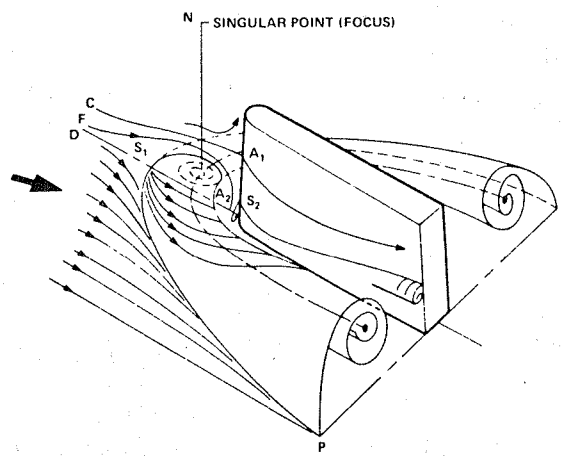

Fig. 10 Sketch of 3-D vortex structure

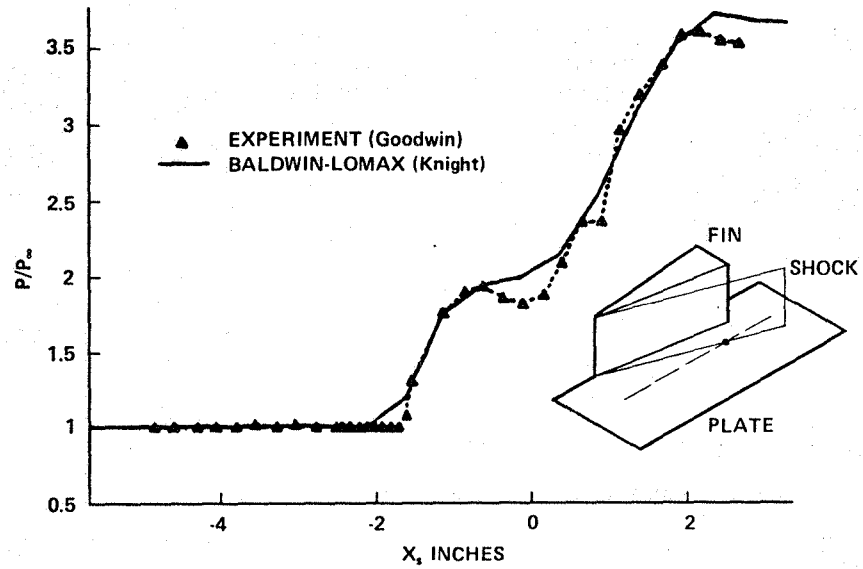

Fig. 11 Comparison of computed and experimental pressure on flat plate for Mach 3 flow over 20° sharp fin at Z = 6.25 cm (Knight)

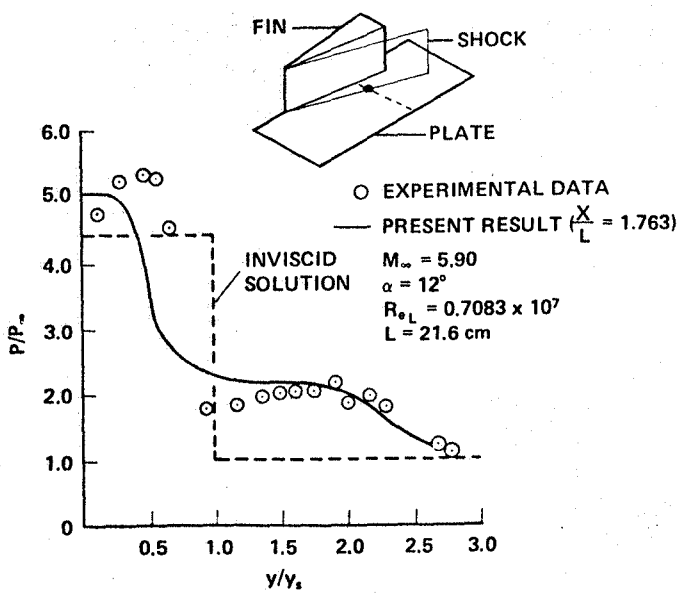

Fig. 12 Comparison of computed and experimental pressure on flat plate for Mach 5.9 12° sharp fin.

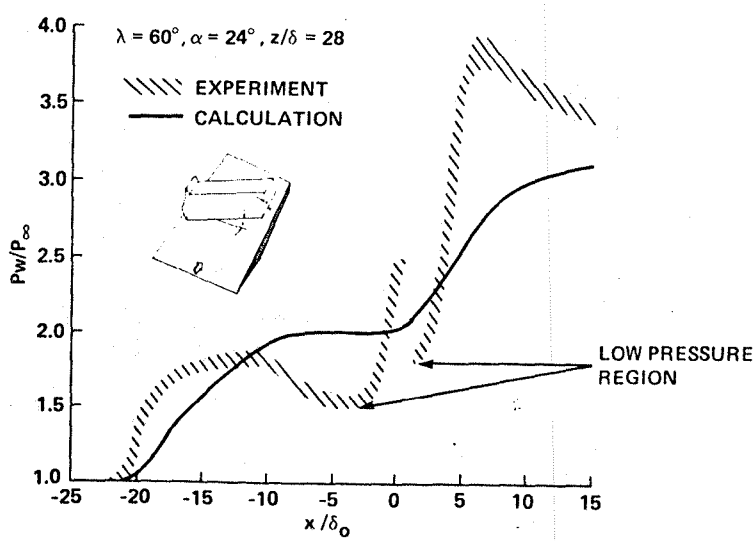

Fig. 13 Comparison of computed and experimental surface pressure along constant Z for Mach 3 over 60° swept wedge (Horstman)

1. Report No.	2. Government Accession No.	3. Recipient's Catalog No.
NASA TM-86780		

4. Title and Subtitle	5. Report Date
COMPUTATION OF THREE-DIMENSIONAL SHOCK WAVE AND BOUNDARY-LAYER INTERACTIONS	August 1985
	6. Performing Organization Code
7. Author(s)	8. Performing Organization Report No.
Ching-mao Hung	85350
	10. Work Unit No.
9. Performing Organization Name and Address	11. Contract or Grant No.
Ames Research Center Moffett Field, CA 94035	
	13. Type of Report and Period Covered
12. Sponsoring Agency Name and Address	Technical Memorandum
National Aeronautics and Space Administration Washington, DC 20546	14. Sponsoring Agency Code 505-31-01

15. Supplementary Notes

Point of Contact: C. M. Hung, MS 202A-1, Ames Research Center, Moffett Field, CA 94035, (415)694-6417 or FTS 464-6417

16. Abstract

Computations of the impingement of an oblique shock wave on a cylinder and a supersonic flow past a blunt fin mounted on a plate are used to study three-dimensional shock wave and boundary layer interaction. In the impingement case, the problem of imposing a planar impinging shock as an outer boundary condition is discussed and the details of particle traces in windward and leeward symmetry planes and near the body surface are presented. In the blunt-fin case, differences between two-dimensional and three-dimensional separation are discussed, and the existence of an unique high-speed, low-pressure region under the separated spiral-vortex core is demonstrated. The accessibility of three-dimensional separation is discussed.

17. Key Words (Suggested by Author(s))	18. Distribution Statement
Three-dimensional separation Shock wave Boundary layer Interaction	Unlimited Star Category: 34

19. Security Classif. (of this report)	20. Security Classif. (of this page)	21. No. of Pages	22. Price*
Unclassified	Unclassified	15	A02

*For sale by the National Technical Information Service, Springfield, Virginia 22161

End of Document